I&EC research
Industrial & Engineering Chemistry Research

Article

pubs.acs.org/IECR

Steady State and Dynamic Operation of Four-Product Dividing-Wall (Kaibel) Columns: Experimental Verification

Deeptanshu Dwivedi,[†] Jens P. Strandberg,[†,¶] Ivar J. Halvorsen,[‡] and Sigurd Skogestad*[,†]

[†]Department of Chemical Engineering, Norwegian University of Science and Technology, Trondheim, Norway
[‡]Applied Cybernetics, SINTEF, Trondheim, Norway

ABSTRACT: Control and operation of energy-efficient dividing-wall columns can be challenging. This paper demonstrates experimentally the start-up and steady state operation of a four-product Kaibel column separating methanol, ethanol, propanol, and *n*-butanol. We use a control structure with four temperature controllers and show that it can handle feed rate disturbances as well as set point changes. The experiments compare well with an equilibrium stage model.

INTRODUCTION

Distillation is a separation technique that uses heat energy to provide the separation work of "un-mixing" the feed mixture. In this paper we study the integrated Kaibel distillation scheme for separation of four components as shown in Figure 1.[2] The main motivation for this scheme is a combination of capital savings and energy savings compared to conventional distillation sequences for multicomponent separation. This scheme is not the best in terms of minimum separation work (exergy), mainly because it performs a difficult B/C split in the prefractionator and not the easiest (A/D) split.

An "ideal reversible" system with minimum exergy requires a more complex arrangement, infinite number of stages and heating and cooling on all stages.[3−5] For four-product separation, Figure 2a shows the reversible scheme proposed by Petlyuk and Platonov.[6] The column sections are directly coupled and the easiest split is done first. Any mixing losses near the feed stage and at the ends can thus be avoided. Some of the features of reversible distillation are retained in an adiabatic "four-product extended Petlyuk column", which has only one heater (reboiler) and one cooler (condenser) (see Figure 2b). In fact, the adiabatic scheme shown in Figure 2b is better than the reversible scheme in Figure 2a in terms of energy although it is inferior in terms of exergy. Compared to conventional two-product column sequences, the potential energy savings in an adiabatic "four-product extended Petlyuk arrangement" (Figure 2b) can be up to 50%.[7] The disadvantage of using the arrangements shown in Figure 2 is that, a large number of sections are required for a multicomponent separation. Petlyuk et al.[1] also proposed schemes for multicomponent separation with a minimum number of column sections. For a four-product separation, one of the schemes given by Petlyuk is the same as the "Kaibel" scheme in Figure 1a.[8]

The four-product Kaibel column in Figure 1, although less efficient than the Petlyuk arrangements in Figure 2, can still offer up to 30% energy saving compared to conventional sequences due to the directly coupled prefractionator.[9] Our experimental setup is similar to the scheme in Figure 1a, which does not have a vertical dividing-wall but the results are extendable to dividing-wall columns.

Numerous successful industrial implementations of three-product dividing-wall columns have been reported by the German company BASF.[10,11] In the open literature, a thorough experimental study for operation of a three-product high purity distillation column was reported by Niggermann et al.[12] Earlier, start-up for a three-product column based on rigorous simulations was reported by Niggermann et al.[13] Mutalib and Smith[14] reported a simulation study on a three-product dividing-wall column and concluded that a conventional proportional-integral (PI) control scheme can give good regulation. They also reported experimental studies done on a pilot plant column.[15] Luyben[16] performed a simulation study and proposed a four-point control structure for a three-product dividing-wall column. van Diggelen et al.[17] compared conventional PID controller with controllers obtained by H_∞ controller synthesis and μ-synthesis. Ling et al.[18] proposed control structures considering remixing losses for an energy optimal operation. Several works have also been reported for the use of model predictive control for dividing-wall columns.[19−21]

There is one reported use of a four-product Kaibel column in BASF and several patents from BASF as summarized by Dejanovic et al.[11] Some simulation work has also been carried out on control and operation of four-product Kaibel columns. Strandberg and Skogestad[22] found in a simulation study that a four-point temperature control scheme with inventory control can stabilize the column and prevent "drift" of the composition profiles during operation. Ghadrdan et al.[23] reported another simulation study on optimal steady state operating solutions for economic criterions like minimizing energy for fixed purity specifications. Kverland et al.[24] studied a multivariable model predictive controller on top of a regulatory layer with a four-point temperature control.

In the open literature, there are no experimental studies reported on operation and control of four-product directly coupled columns. In this paper we present experimental results for a four-product Kaibel column separating methanol, ethanol,

Received: May 31, 2012
Revised: October 21, 2012
Accepted: November 7, 2012
Published: November 7, 2012

ACS Publications © 2012 American Chemical Society

dx.doi.org/10.1021/ie301432z | *Ind. Eng. Chem. Res.* 2012, 51, 15696−15709

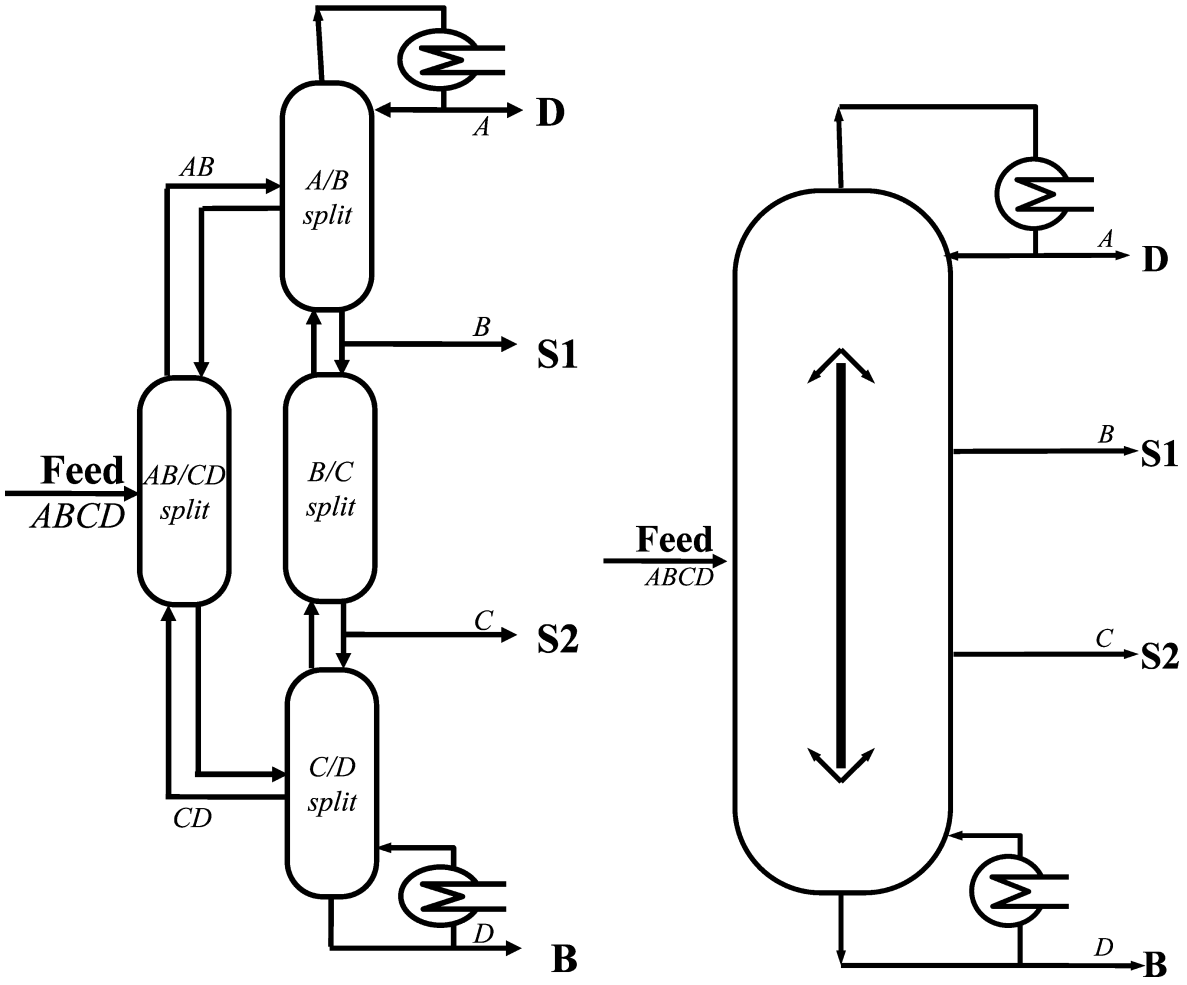

Figure 1. Thermodynamically equivalent implementations of four-product Kaibel column (studied in this paper).

1-propanol, and 1-butanol (with normal boiling points of 64.7 °C, 78.4 °C, 97.2 °C, and 117.7 °C, respectively).

EXPERIMENTAL SETUP

Figure 3a shows a picture of our experimental column.[25] Although this is not a dividing-wall column, it is thermodynamically equivalent as illustrated in Figure 1. The height of the column is about 8 m. The system is operated at atmospheric pressure and the column sections are packed with 6-mm glass Raschig rings. The column sections are numbered from 1 to 7 as shown in Figure 3a. Sections 1 and 2 constitute the prefractionator, while sections 3−7 form the main column. The internal diameter of vacuum jacket glass column-sections 1, 2, 4, 5, and 6 is 50 mm while that of column-sections 3 and 7 is 70 mm (column sections are numbered in Figure 3c). The height of packing in sections 1 and 2 is 1.1 and 1.6 m, respectively, while in sections 3, 4, and 5 it is 0.65 m. The height of packing in sections 6 and 7 is about 0.75 m and 0.9 m, respectively.

The reboiler is kettle type and the power to the reboiler is adjusted by varying the voltage to the heater elements through a thyristor. The condenser is mounted on top of the column and is water-cooled. The condensed vapor flows back to the column due to gravity; a part is taken out as top product and the rest forms the liquid reflux.

The liquid reflux split valve, top product valve, and side product valve are swinging funnels (on/off) and are controlled by externally placed solenoids. The flow through the swinging funnel depends on the internal liquid flows in the respective column section. To implement the continuous output of the proportional-integrator (PI) controllers, the common technique of pulse width modulation (PWM) is used where the width (length of the pulse is the adjustable continuous variable) and the period (cycle time) is normally fixed. The cycle time of the on/off valves should be much shorter than the plant time constant and hence emulate continuous-pump like flow conditions. In our case, the valve switching function has a total cycle time about 10 s and a resolution time for switching of 0.2 s. For example, if the controller output is 0.22, a valve position on one side of the funnel is 2.2 and 7.8 s on the other. This gives an implemented accuracy of 4% when the valve position is 0.5, but much worse resolution when close to the fully open (0)/ close (1) position. To improve the resolution, we used an algorithm that allows also the total cycle time to change between 5 and 15 s. This implementation reduces the rounding off errors and improves the resolution of the valve.

In our setup, it is also possible to adjust the vapor split ratio (R_V) between the prefractionator and the main column using a valve, but in the reported experiments it has been kept constant as is common in industrial implementations. The vapor split between the prefractionator and the main column is then determined by the normal pressure drop offered by the packing in the column sections.

The liquid-level measurement in the reboiler was faulty and a level controller could not be installed. Therefore, the bottom

dx.doi.org/10.1021/ie301432z | Ind. Eng. Chem. Res. 2012, 51, 15696−15709

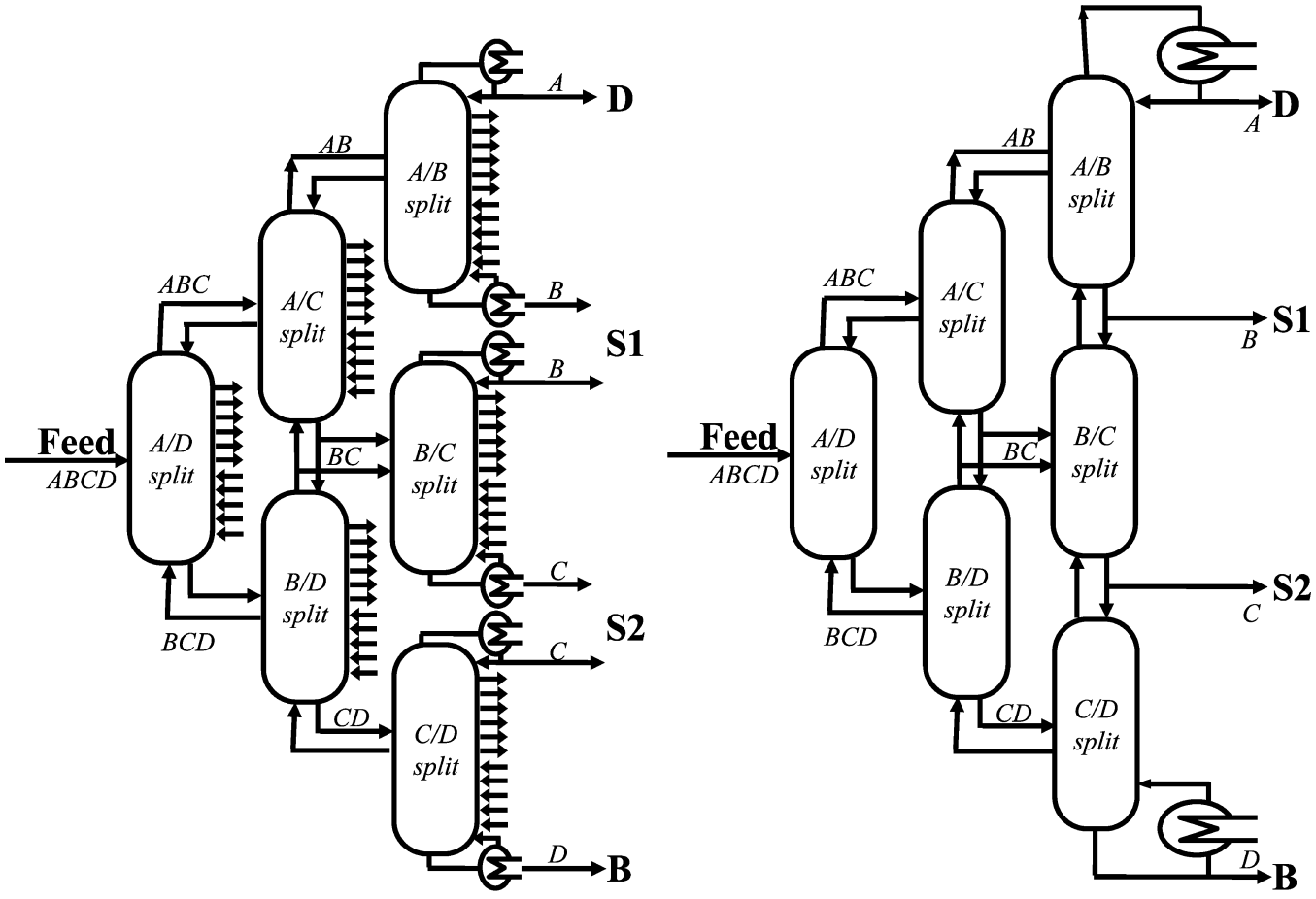

(a) *Four-product "reversible" Petlyuk column* (b) *Four-product adiabatic Petlyuk column*

Figure 2. "Reversible" and adiabatic arrangements of Four-product "extended" Petlyuk column (*not* studied in this paper).

product was allowed to accumulate during the experimental runs. With a large reboiler, the composition of the bottoms will then take a long time to reach steady state, but otherwise this should have little effect on the experimental results.

The control setup is implemented in Lab View on a standard PC. Figure 4 is a screen-shot from the computer interface (Lab View) during the experimental run 12, with a snapshot of temperatures as read by the probes in various sections. The dialogue labeled "Temperature graphs" shows the four controlled temperatures for 100 s. Note that some of the temperature measurements have large measurement biases (for example, TP4 and T16) and their values are calibrated for later analysis and one probe (T15) is faulty.

CONTROL STRUCTURE

As reported in the simulation study earlier by Strandberg and Skogestad,[22] a 4-point temperature control structure can avoid "drift" of the composition profile in the various sections of a 4-product column. Temperature is a good indicator of composition and is easy to measure. Temperature control is fast and can keep the compositions (and split) in the column close to nominal value and hence preventing "drift" in the event of disturbances.

In Figure 3c, we show the control structure used in the experiments. In Table 1, we show in more detail the loop pairings. The four temperature control loops are named loop 1, 2, 3, and 4. In the footnote to Table 1, we also define the four corresponding liquid flow ratios R_{L1}, R_{L2}, R_{L3}, and R_{L4} which are set by the swinging funnels.

In control loop 1, the liquid split ratio (R_{L1}) is used to control a sensitive temperature in the prefractionator (T_2 = TP5). In loop 2, the distillate split ratio (R_{L2}) controls a temperature in section 3 (T_3 = TM3). In the loop 3, the upper side product split ratio (R_{L3}) controls a sensitive temperature in section 5 (T_5 = TM8). Finally, in control loop 4, the lower side product split ratio (R_{L4}) is used to control a sensitive temperature in the bottom section (T_7 = TM14).

The controllers are conventional proportional-integrator (PI) controllers. As the system is interactive, we used sequential tuning, and loop 1 in the prefractionator was closed first. Next loops 2, 3, and 4 in the main column were closed. The tuning of the loops was done using the SIMC rules[26] with the tuning parameter, τ_C, chosen to be 1 min for loops 1 and 2 and 2 min for loops 3 and 4. The temperature set points for the loops were adjusted during start-up as explained below.

The remaining two degrees of freedom, the boilup (V) and the vapor split ratio (R_V), are not used for control in experiments, but may be in general available for some optimizing objective, like minimizing energy for a given specification.

EXPERIMENTS

Various experiments were conducted for studying the start-up operation, to test the 4-point control structure for set point changes, disturbance handling and to study steady state

dx.doi.org/10.1021/ie301432z | *Ind. Eng. Chem. Res.* 2012, 51, 15696−15709

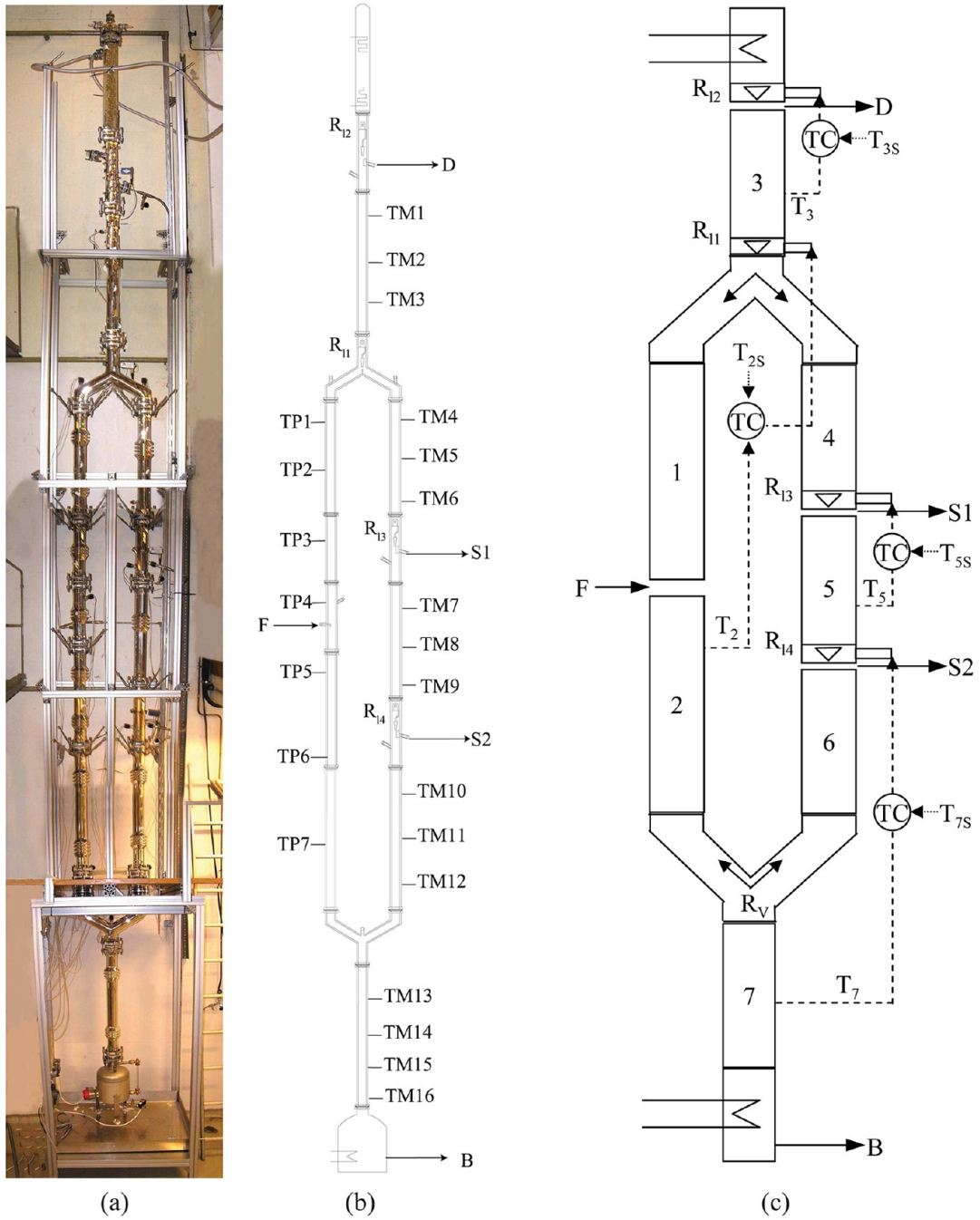

Figure 3. (a) Picture of the experimental column.[25] (b) Schematic showing location of temperature sensors.[25] (c) 4-Point regulatory control structure used for operation T_2 = TP5, T_3 = TM2, T_5 = TM8 and T_7 = TM14.

operation. Table 2 shows a list of the 13 experiments reported in this paper.

Start-up. Figure 5a shows the results from a typical cold start-up of the pilot plant (experimental run 1). The following start-up policy was used:

After turning on the reboiler (at time =0), the column is heated up in total reflux mode ($D = 0$, S1 = 0, S2 = 0, $F = 0$). Initially, the output of control loop 1 (R_{L1}) is fixed at a reasonable value (manual mode). In our case, it was fixed at $R_{L1} = 0.3$ which implies that 30% of the reflux is directed to the prefractionator and 70% to the main column. The output of R_{L2}, R_{L3}, and R_{L4} of control loops 2, 3, and 4 were initially fixed at 1 (no product withdrawal). At about 30 min, the feed to the column is turned on. Shortly after, the controllers (loops 1, 2, 3, and 4) are turned on (AUTO mode). With control loops 2, 3, and 4 turned on, we begin to draw the three products D, S1, and S2. The initial temperature set points are the values from the total reflux mode, and the set points are then adjusted in closed-loop mode to get good separation in the column. The temperature set point for the prefractionator (T_{2s}) is adjusted to get a large temperature change across the prefractionator column. This corresponds to a sharp split between the intermediate components (ethanol and propanol). The set points for the remaining loops (T_{3s}, T_{5s}, and T_{7s}) are for the main column which performs binary splits, and these are adjusted in an attempt to get the temperatures of the four product close to the normal boiling point of their

dx.doi.org/10.1021/ie301432z | Ind. Eng. Chem. Res. 2012, 51, 15696−15709

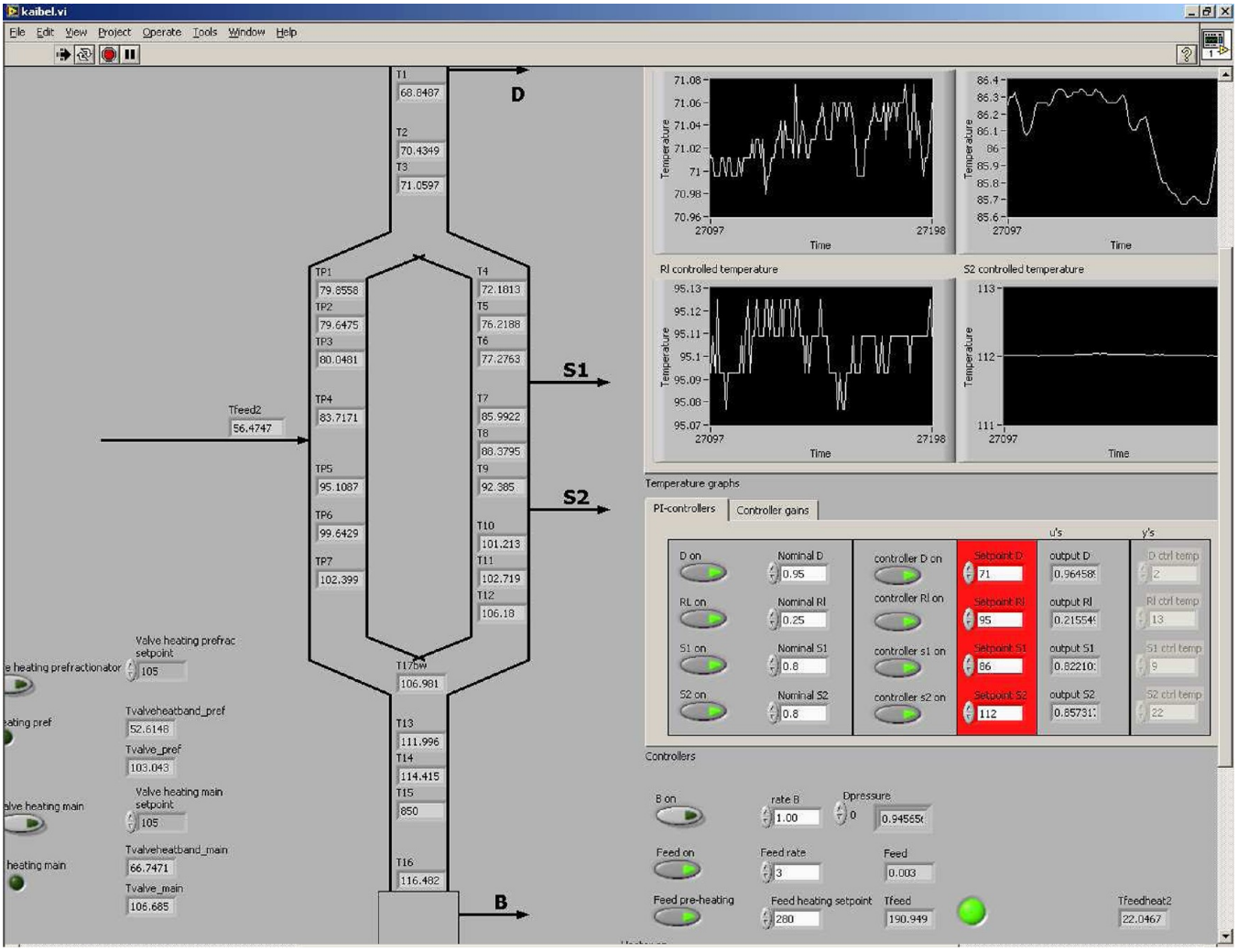

Figure 4. Screen-shot of operator interface during experimental run 12.

Table 1. Four-Point Temperature Regulatory Control Structure[a,b]

control loop	manipulated variable[a]	controlled variable[b]
loop 1	liquid split valve (R_{L1})	temperature in section 2 (T_2)
loop 2	distillate split valve (R_{L2})	temperature in section 3 (T_3)
loop 3	upper side product split valve (R_{L3})	temperature in section 5 (T_5)
loop 4	lower side product split valve (R_{L4})	temperature in section 7 (T_7)

[a]Manipulated variables (controller outputs) are the swinging funnel ratios R_{L1}, R_{L2}, R_{L3}, and R_{L4}: $R_{L1} = L_1/L_3$, $R_{L2} = L_3/(L_3 + D)$, $R_{L3} = L_5/(L_5 + S1)$, $R_{L4} = L_6/(L_6 + S2)$. Here, L_1, L_3, L_5, and L_6 are liquid flows in sections 1, 3, 5, and 6, respectively (see Figure 3). S1 and S2 are side product flow rates. [b]Controlled variables are temperature sensors as shown in Figure 3b,c. T_2 = TP5, T_3 = TM3, T_5 = TM8, and T_7 = TM14

corresponding main components. Off-line analysis of the products (reported later) shows that this start-up procedure resulted in good quality products, in spite of the fact that we used only temperature loops. Of course, if online composition measurements are available, these should be used to adjust the temperature set points.

Figure 5b shows a zoomed-in plot of Figure 5a for the time period from 35 to 140 min. In the experiments, the feed flow rate was held constant at 3 L/hour and the reboiler duty was set constant at 2 kW. We conclude from the experiment (Figure 5a,b) that the start-up procedure works well and leads to stable operation.

Closed-Loop Operation. In the following experiments (runs 2−7), the four temperatures set points are changed in closed-loop, to drive the system to various new steady states. The composition of the feed mixtures is also varied.

In Figure 6 (run 2), we show results for a temperature set point change of −2 °C to control loop 1. This set point change can be handled well and the steady state is reached in about 25 min. There is an initial delay of about 1 min as the location of the temperature is far from the valve. As a consequence, it takes a while for the change in the liquid reflux to affect the controlled temperature. This loop has interactions with loops 3 and 4, as T_5 (measured) and T_7 (measured) show some deviation from their set points due to action of R_{L1}.

Figure 7 (run 3) shows a set point change of ±1 °C change in the loop 2. Again, this set point change is handled well. However, there is significant interaction with all the other loops. This is

dx.doi.org/10.1021/ie301432z | Ind. Eng. Chem. Res. 2012, 51, 15696−15709

Table 2. List of Experiments[a]

experiment	description
run 1	cold start-up
run 2	−2 °C set point change in T_2 (prefractionator loop)
run 3	±1 °C set point changes in T_3 (distillate product loop)
run 4	±1 °C set point changes in T_5 (upper side product loop)
run 5	±1 °C set point changes in T_7 (lower side product loop)
run 6	simultaneous ±1 °C set points changes in all temperatures
run 7	+20% disturbance in feed rate
run 8	steady state run with constant set points: T_2 = 80.6 °C, T_3 =69 °C, T_5 = 82 °C, T_7 = 110.2 °C
run 9	steady state run with constant set points: T_2 = 88 °C, T_3 = 69 °C, T_5 = 88 °C, T_7 = 113 °C
run 10	steady state run with constant set points: T_2 = 91 °C, T_3 = 69.5 °C, T_5 = 92 °C, T_7 = 113 °C
run 11	steady state run with constant set points: T_2 = 91.5 °C, T_3 = 72 °C, T_5 = 92 °C, T_7 = 112 °C
run 12	steady state run with constant set points: T_2 = 95 °C, T_3 = 71 °C, T_5 = 86 °C, T_7 = 112 °C
run 13	total reflux experiment for calculating number of theoretical stages

[a]Feed rate for all runs (except run 7) = 3 LPH. Reboiler duty for all runs = 2 kW.

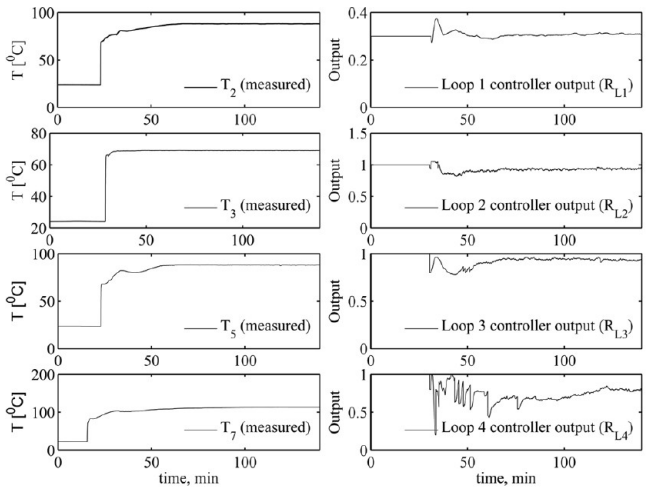

(a) *Cold Start-up: Entire run*

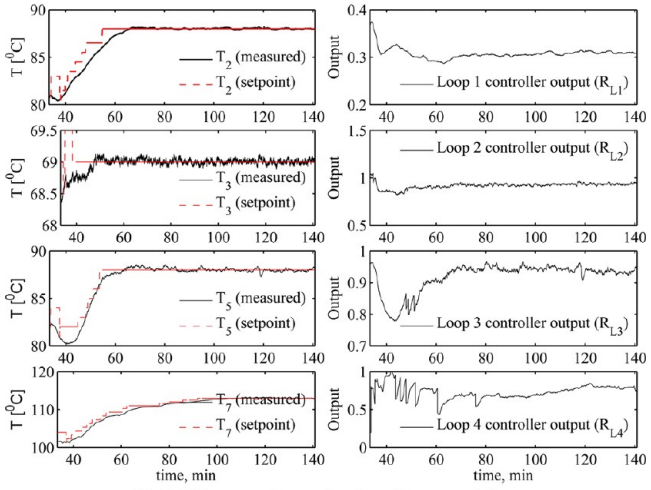

(b) *Cold Start-up (Zoomed in from 35 min to 140 min*

Figure 5. Experimental run 1: Cold start-up.

because a change in distillate flow affects directly the molar difference between the boilup (V) and liquid reflux (L) in the entire column.

Figures 8 and 9 (runs 4 and 5) plot show similar set point changes in loops 3 and 4, respectively, and these changes are handled well without interactions with other loops. Figure 10 (run 6) shows simultaneous changes in the set point for all the four loops, which are also handled reasonably well.

Finally, Figure 11 (run 7) shows the response for an increase in feed rate from 3 L/h to 3.6 L/h (+20%). This disturbance can also be handled well, and the controlled-temperatures are brought back to their set points in about 30 min.

Steady State Experiments and Comparison with Simulations. To study the steady-state behavior, experimental runs 8−12 were carried out with constant temperature set points. For runs 9−12, samples of the feed and products were collected and analyzed using high-performance liquid chromatography (HPLC). Figure 12 (run 8) shows a typical response when the column is "steady" for a period of 2 h, with all the four temperature loops closed. All the four temperatures can be maintained at their respective set points. The steady-state results for run 9−12 are summarized in Table 3 (compositions) and Table 4 (controller outputs ≡ plant inputs).

We now want to compare the steady-state experimental results with a standard equilibrium stage distillation model. The vapor−liquid equilibria is modeled using the Wilson model for the liquid phase, and the vapor is assumed to be ideal. We use the constant molar overflow assumption, which is reasonable for our mixture (see Appendix for details of the dynamic model, but note that, we have compared only the steady state experiments with the model).

To match the experimental steady state data, we can adjust the following degrees of freedom in the model:

1. theoretical number of stages (we use a fixed value for all experiments)
2. boilup (V/F)
3. feed composition
4. liquid split ratio (R_{L1})
5. vapor split ratio (R_V)
6. distillate product split ratio (R_{L2})
7. upper side product split ratio (R_{L3})
8. lower side product split ratio (R_{L4})

The degrees of freedom are adjusted for each experiment, except for the theoretical number of stages in the sections. The number of theoretical stages was based on experimental estimation of height equivalent of a theoretical plate (HETP). For the estimation of HETP, a total reflux experiment (run 13) was performed with only two components, namely methanol and ethanol. The liquid split ratio (R_{L1}) was used to control temperature difference ($\Delta T = T_2 - T_5$) between the prefractionator (section 2) and the main column (section 5). The temperatures ($T_2 \equiv$ TP5, $T_5 \equiv$ TM8) chosen were approximately at the same height (and of packing) from the reboiler. The set point of this controller was then set to *zero* so that the compositions should be the same on both sides. The system was allowed to stabilize and samples were taken at the location of side products (S1 and S2) for analysis. Figure 13 shows the stable run during this experiment with the controlled-variable (ΔT) and controller output. The molar composition of methanol was about 75% and 21% in samples S1 and S2, respectively. The graphical McCabe Thiele method and Fenske equation both give the number of theoretical stages to be about 4.

dx.doi.org/10.1021/ie301432z | *Ind. Eng. Chem. Res.* 2012, 51, 15696−15709

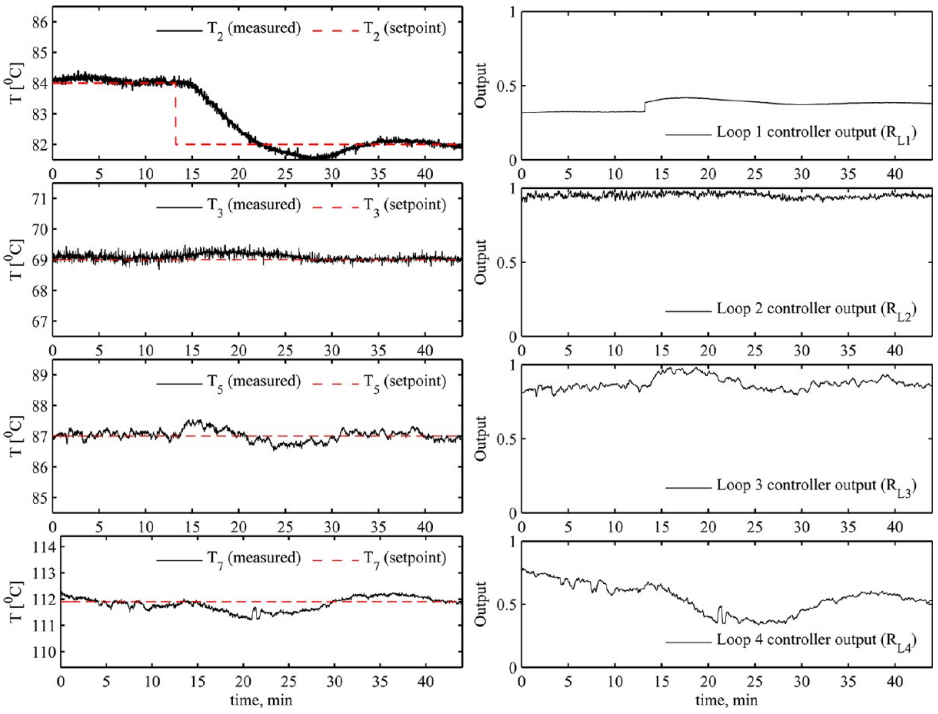

Figure 6. Experimental run 2: −2 °C set point change in prefractionator temperature, T_2 (control loop 1).

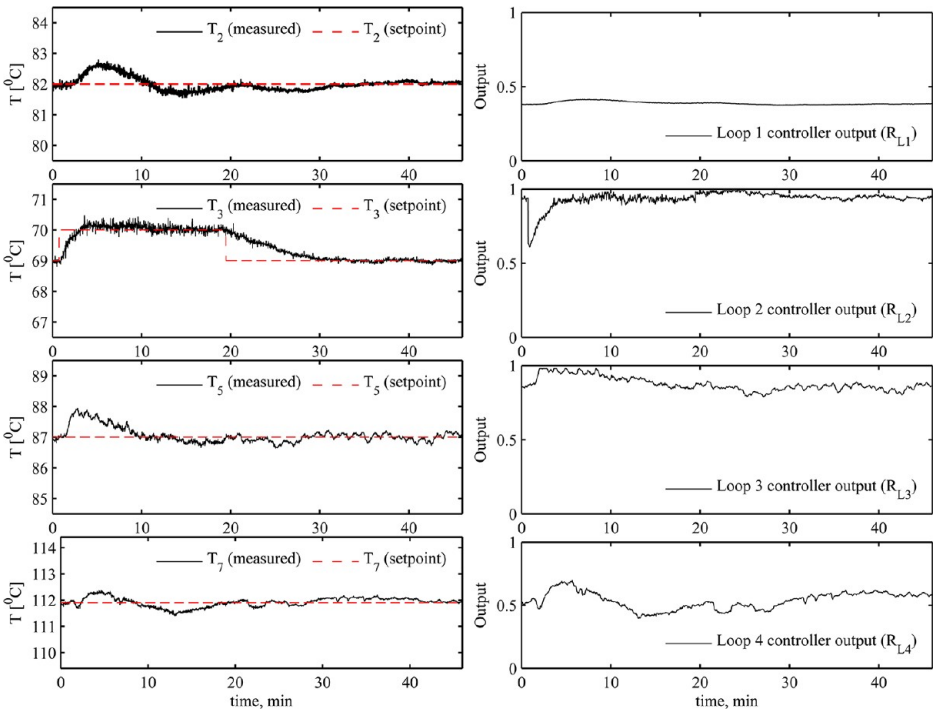

Figure 7. Experimental run 3: ±1 °C set point change in top section temperature, T_3 (control loop 2).

The height of packing between the sample points is 0.65 m and, the HETP for our packing was thus estimated to be about 16 cm. The value of HETP = 16 cm was used to find the number of stages in each section which gives 17 (7 + 10) theoretical stages for the prefractionator and 22 (4 + 4 + 4 + 4 + 5 + reboiler) for the main column.

Based on the power input of 2 kW to the reboiler, we can obtain the boilup (V/F) for use in the model. The feed composition is available from HPLC measurements. Finally, the liquid split ratio (R_{L1}) was obtained directly from the experiments.

With the first *four* degrees of freedom determined (i.e., theoretical number of stages, boilup, feed composition, and liquid split ratio), we are left with *four* more degrees of freedom (vapor split ratio R_V, distillate product split ratio R_{L2}, upper side product split ratio R_{L3} and lower side product split ratio R_{L4}), which are adjusted to match the following experimental values from the steady state runs:

dx.doi.org/10.1021/ie301432z | *Ind. Eng. Chem. Res.* 2012, 51, 15696−15709

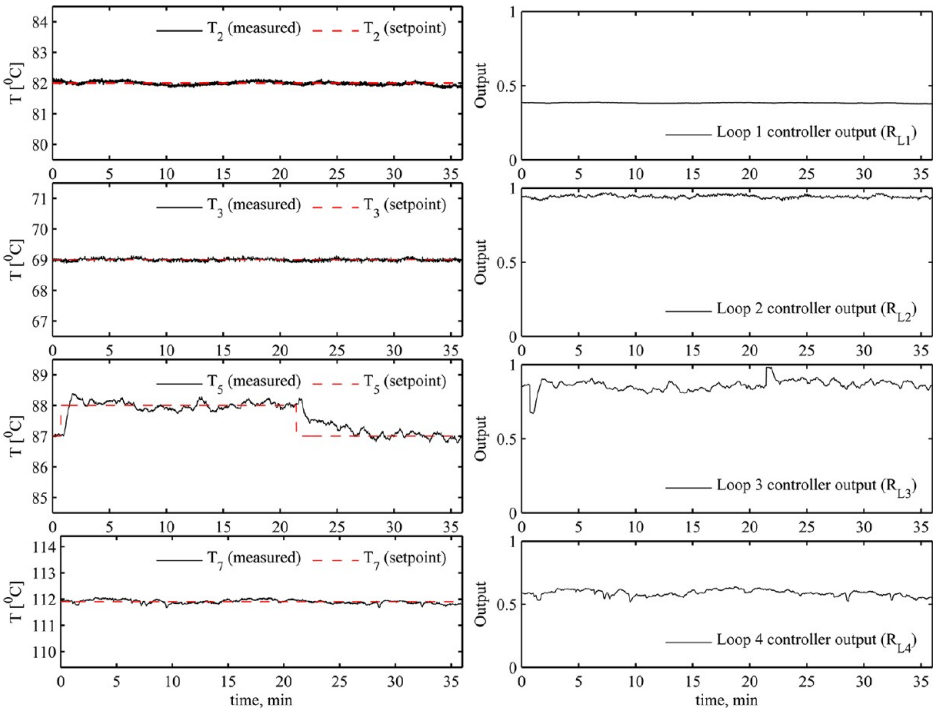

Figure 8. Experimental run 4: ±1 °C set point change in middle section temperature, T_5 (control loop 3).

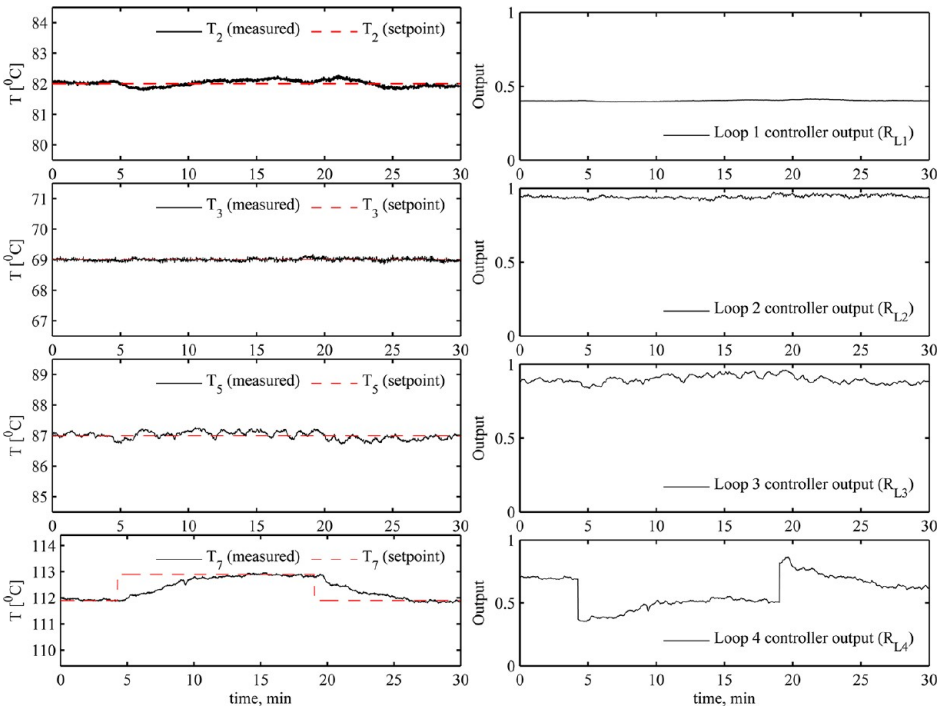

Figure 9. Experimental run 5: ±1 °C set point change in bottom section temperature T_7 (control loop 4).

1. mole fraction of methanol in the top product (D)
2. mole fraction of ethanol in the upper side product (S1)
3. mole fraction of propanol in lower side product (S2)
4. a temperature in section 2 (TP5) of the prefractionator

This procedure for data fitting is used for experimental runs 9–12. Table 3 compares the product composition from experiments and simulations and Table 4 gives the corresponding values of the four degrees of freedom. Since the mole fractions of the main components in the top product (D), upper side product (S1), and lower side product (S2) are matched directly, there is an exact match of these compositions. But additionally, the key impurities in the side products (S1 and S2), which were not matched individually, show a very good fit. For example, in experimental run 9, the mole fraction of methanol in S1 from the experiment is 31.8%, while from the simulation it is 34.2%. The key impurities (propanol and *n*-butanol) of the lower side product (S2) also show a good fit. From Table 4, we see that the simulated values of the four degrees of freedom (R_{L1}, R_{L2}, R_{L3},

dx.doi.org/10.1021/ie301432z | *Ind. Eng. Chem. Res.* 2012, 51, 15696–15709

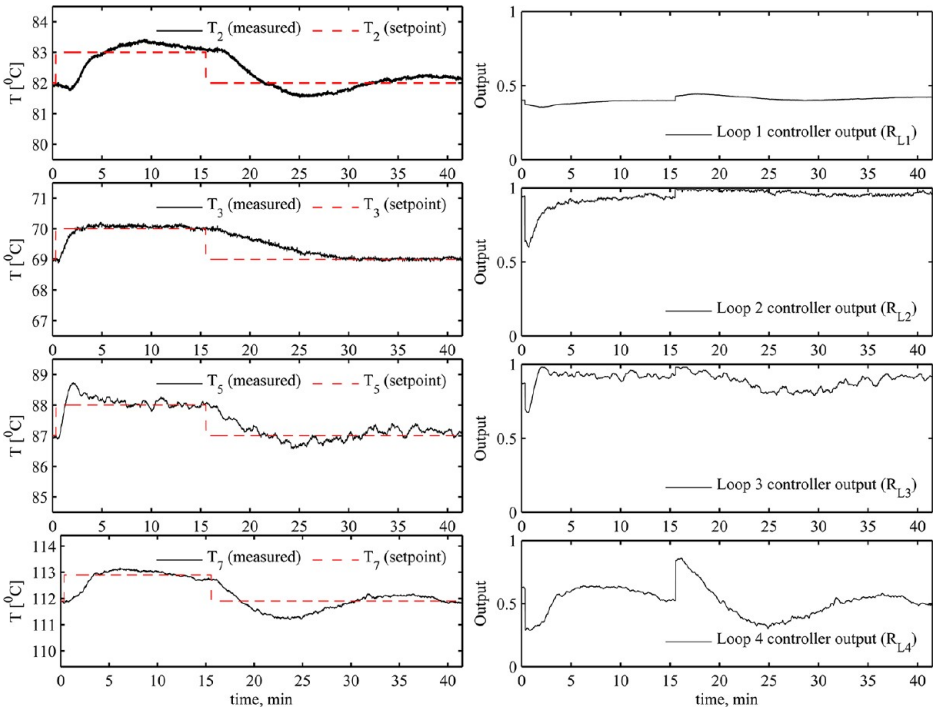

Figure 10. Experimental run 6: Simultaneous change in all four temperature set points.

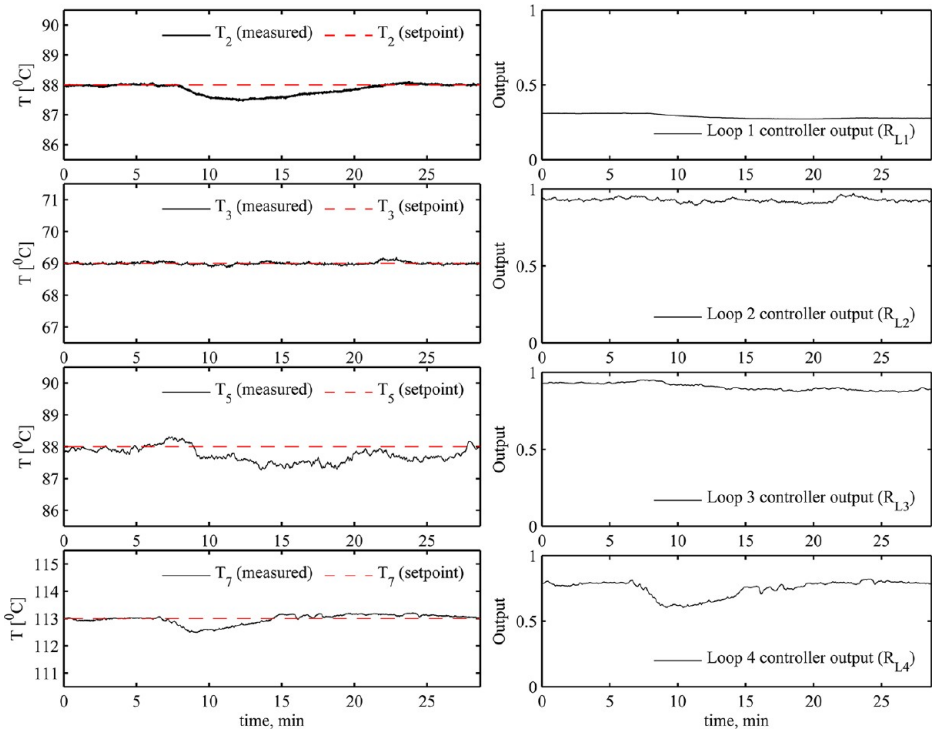

Figure 11. Experimental run 7: +20% feed rate disturbance (at t = 5 min).

and R_{L4}) which were obtained by matching the compositions, agree well with the experimental values.

Figure 14 compares the temperatures from the model (lines) and the experiments (points). The y-axis in Figure 14 shows the theoretical stages in the model, numbered from top (1) to bottom (22). The x-axis shows the corresponding temperatures. The locations of temperature probes in the experimental setup with respect to the theoretical stages in the model are not precise and were not adjusted, but nevertheless we find that the match is good.

In summary, we have a very good agreement between the experimental steady-state data and the equilibrium stage model.

DISCUSSION

Practical Issues Related to Operation. The operation of the experimental column had some problems. Early on, the

dx.doi.org/10.1021/ie301432z | Ind. Eng. Chem. Res. 2012, 51, 15696−15709

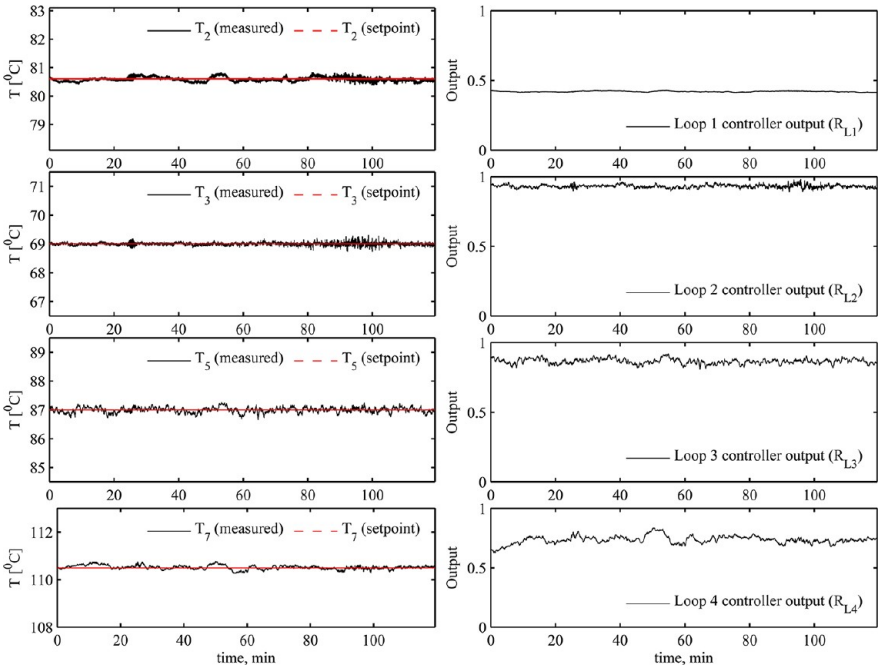

Figure 12. Experimental run 8: steady state operation (T_{2S} = 80.6 °C, T_{3S} = 69 °C, T_{5S} = 82 °C and T_{7S} = 110.2 °C).

Table 3. Steady State Experimental and Simulated Compositions in Runs 9−12

	feed	D		S1		S2		B	
component	expt and sim	expt	sim	expt	sim	expt	sim	expt	sim
				Experiment Run 9					
methanol (mol %)	**21.4**	**96.6**	**96.6**	31.8	34.2	0	1.3	0	0
ethanol (mol %)	**15.4**	3.4	3.4	**55.4**	**55.4**	16.8	15.4	0	0
propanol (mol %)	**21.4**	0	0	12.7	10.3	**75.0**	**75.0**	7.4	1.8
n-butanol (mol %)	**41.7**	0	0	0	0	8.2	8.3	92.6	98.2
				Experiment Run 10					
methanol (mol %)	**20.4**	**94.9**	**94.9**	29.9	27.4	0	0.6	0	0
ethanol (mol %)	**27.4**	5.1	5.1	**51.2**	**51.2**	5.9	6.6	0	0
propanol (mol %)	**28.5**	0	0	18.9	21.3	**87.5**	**87.5**	4.6	2.43
n-butanol (mol %)	**23.7**	0	0	0	0	6.6	5.3	95.4	97.6
				Experiment Run 11					
methanol (mol %)	**20.4**	**92.7**	**92.7**	17.3	14.8	0	0.2	0	0
ethanol (mol %)	**17.6**	7.3	7.3	**51.5**	**51.5**	5.4	4.6	0	0
propanol (mol %)	**26.7**	0	0	31.2	33.5	**89.6**	**89.6**	6.7	3.1
n-butanol (mol %)	**35.3**	0	0	0	0.1	4.9	5.6	93.3	96.9
				Experiment Run 12					
methanol (mol %)	**16.3**	**94.4**	**94.4**	26.3	22.3	0	0.5	0	0
ethanol (mol %)	**19.0**	5.6	5.6	**56.3**	**56.3**	10.1	7.3	0	0
propanol (mol %)	**28.3**	0	0	17.3	21.3	**86.3**	**86.3**	6.4	2.7
n-butanol (mol %)	**36.4**	0	0	0	0	3.5	5.8	93.6	97.2

Table 4. Degree of Freedom in the Four Experiments 9−12

	run 9		run 10		run 11		run 12	
degree of freedom	expt	sim	expt	sim	expt	sim	expt	sim
R_{L1}	**0.31**	**0.31**	**0.15**	**0.15**	**0.25**	**0.25**	**0.22**	**0.22**
R_{L2}	0.93	0.95	0.98	0.98	0.93	0.95	0.96	0.97
R_{L3}	0.94	0.90	0.72	0.81	0.81	0.86	0.83	0.88
R_{L4}	0.75	0.87	0.83	0.91	0.90	0.91	0.86	0.88
R_V		0.39		0.30		0.35		0.32

column was very difficult to operate and stabilize with little material reaching the top of the column.[25] On the intuition that suggested that this was due to insufficient boilup, the reason turned out to be vapor leaking from the product valves on the side streams. To resolve this issue, we installed an additional small manual valve and a solenoid valve (in series) downstream

dx.doi.org/10.1021/ie301432z | Ind. Eng. Chem. Res. 2012, 51, 15696−15709

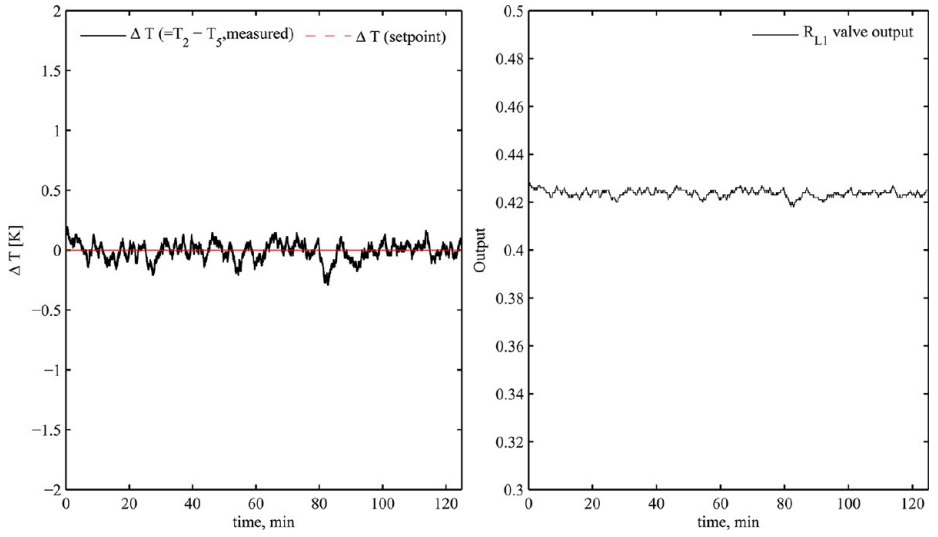

Figure 13. Experimental run 13: total reflux conditions for determining the HETP.

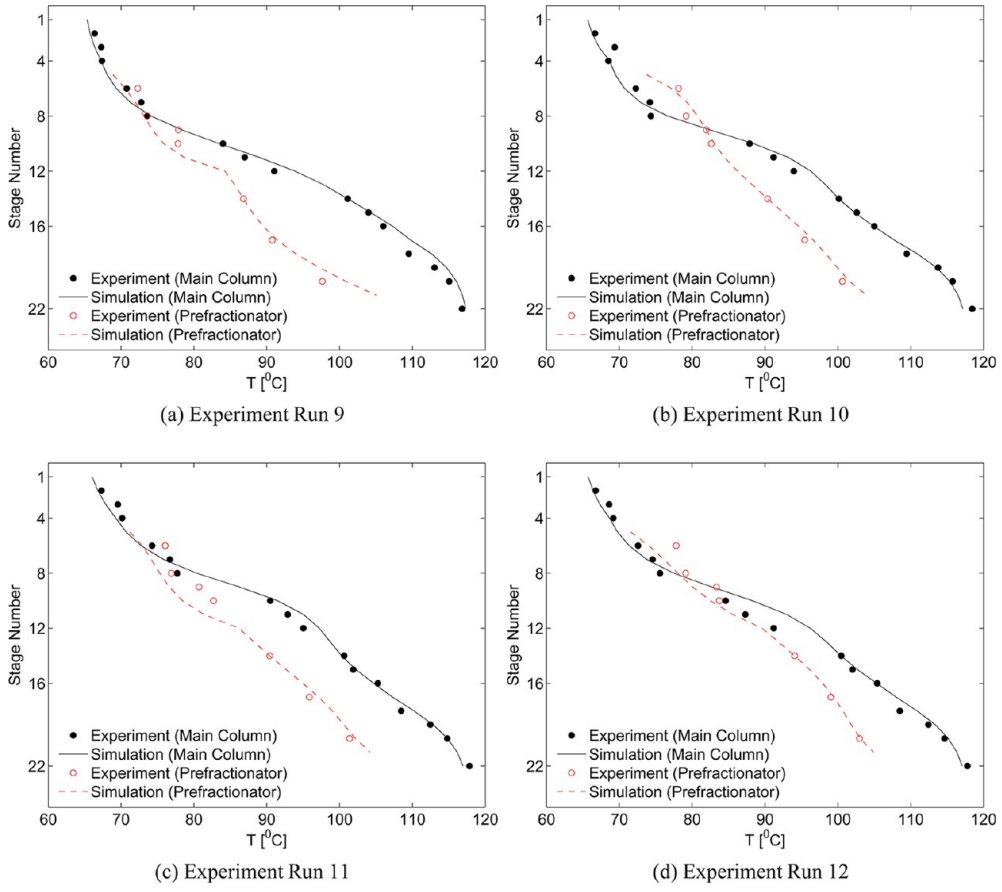

Figure 14. Steady state experimental and simulated temperature profiles in experiments 9−12.

of the swinging funnels, just outside the column. The opening of the manual valve was adjusted to ensure that there was always a liquid hold up in the glass downcomer under the swinging funnel. The additional solenoid valves and the swinging funnel open and close simultaneously during the cycle. Alternatively, an externally placed liquid seal in the product withdrawal line would have stopped any vapor from "leaking" by providing a hydraulic head to counter the small positive pressure in the column.

Plant-Model Mismatch. As mentioned, the equilibrium stage model fits well with the experiments. The mole fraction of butanol in the bottoms product was, however, smaller than that in the model in all the runs. One reason for this may be that we have no bottom product (B), meaning that the bottom product accumulates in the reboiler, and therefore it will take a very long time to reach the steady compositions in the reboiler.

The experimental data also had some uncertainties. The experimental results for example in Figure 12, show some noise

dx.doi.org/10.1021/ie301432z | Ind. Eng. Chem. Res. 2012, 51, 15696−15709

Table 5. Operation under Two Optimal Modes[a]

	mode I	mode II
objective	$J = x^{S1}_{EtOH} + x^{S2}_{PrOH}$	$J = x^{D}_{MeOH} + x^{S1}_{EtOH} + x^{S2}_{PrOH} + x^{B}_{BuOH}$
degrees of freedom	liquid split ratio, R_{L1}	R_{L1}
	distillate split ratio, R_{L2}	R_{L2}
	upper side product split ratio, R_{L3}	R_{L3}
	lower side product split ratio, R_{L4}	R_{L4}
	Vapor split ratio, R_V	R_V
constraints	boilup = nominal	boilup = nominal
	feed rate = nominal	feed rate = nominal
	feed composition = nominal	feed composition = nominal
	feed liquid fraction = nominal	feed liquid fraction = nominal
	x^{D}_{MeOH} = nominal	
	x^{B}_{BuOH} = nominal	

[a]The remaining degrees of freedom are used for liquid and vapor inventory control, and hence are not available as degrees of freedom for optimization. The bottoms rate and distillate flow are consumed for level control of reboiler and condenser, respectively; Condenser duty is used for pressure control.

in the temperatures. This can be just instrument noise or process noise due to the use of swinging funnels and not continuous valves with pumps. The composition measurements with HPLC also have some measurement error. There were some biases in temperature probes. These were calibrated using their measurements in cold column conditions. Some probes showed up to 3 °C of error from the room temperature and their measurements were accordingly corrected.

Another source of error can be the column pressure drop, which was neglected in the model. The total pressure drop under normal operation of the column was about 16 cm of water or about 0.016 bar (measured using a U-tube manometer).

Optimal Operation. From the experimental data and the model in Table 3, the purities of top and bottom products are relatively high (up to about 96% and 95%), while the purities of the side products are low (about 55% and 89%). Is this the best one can achieve? To answer this question, we used the model to compare the four experimental steady-state runs to operations under two "optimal" modes.

In mode I, for a given boilup and with the purity of top product (x^{D}_{MeOH}) and bottom product (x^{B}_{BuOH}) specified, the objective is to maximize the sum of the purities of the side products. In mode II, also for a given boilup, the objective is to maximize the sum of purities of all the products.

The two optimization problems (mode I and mode II) are defined in more detail in Table 5 and the results are given in Table 6. Table 6 compares the product purities in the four experimental runs with the "optimal" values in modes I and II. In mode I, where the top and bottom purities are fixed, we find that some minor improvement can be made in the side stream purities. The largest difference is in experimental run 11, where the S1 purity can be improved from 51.5% to 65.4%. On the other hand, in runs 10, 11, and 12, the S2 purity is actually better in the experiment.

In mode II, even though there was an improvement on the sum of the purities of four products, the purity of the end products (D and B) decreased from the base case. The purity of the upper side products (S1) increased in all the scenarios while the purity of lower side product (S2) decreased in experimental runs 11 and 12.

From the results in Table 6, we conclude that the experimental results are close to "optimal" operations, as described by mode I or mode II. This shows that the temperature set point adjustment procedure described in the start-up procedure works well.

Table 6. Comparison of Experiments 9−12 with Optimal Operation in Mode I (Maximize Sum of the Purities of Side Products) and Mode II (Maximize Sum of the Purities of All the Products)

	D			S1			S2			B		
		mode			mode			mode			mode	
component	expt	I	II	expt	I	II	expt	I	II	expt	I	II
						Experiment Run 9						
methanol	96.6	96.6	89.7	34.2	28.9	13.0	1.3	0.7	0.4	0.0	0.0	0.0
ethanol	3.4	3.4	10.2	55.4	52.9	71.2	15.4	10.1	13.4	0.0	0.0	0.0
propanol	0.0	0.0	0.0	10.3	18.1	15.9	75.0	80.8	82.2	1.8	1.8	3.5
butanol	0.0	0.0	0.0	0.0	0.1	0.0	8.3	8.4	4.0	98.2	98.2	96.5
						Experiment Run 10						
methanol	94.9	94.9	94.6	27.4	29.2	27.1	0.6	0.7	0.6	0.0	0.0	0.0
ethanol	5.1	5.1	5.3	51.2	53.6	53.6	6.7	8.6	7.7	0.0	0.0	0.0
propanol	0.0	0.0	0.0	21.4	17.1	19.2	87.5	85.5	88.0	2.4	2.4	3.5
butanol	0.0	0.0	0.0	0.1	0.1	0.0	5.3	5.1	3.6	97.6	97.6	96.5
						Experiment Run 11						
methanol	92.7	92.7	92.9	15.3	18.3	18.8	0.2	0.5	0.5	0.0	0.0	0.0
ethanol	7.3	7.3	7.1	51.5	65.4	64.2	4.4	11.7	10.9	0.0	0.0	0.0
propanol	0.0	0.0	0.0	33.0	16.2	16.9	89.6	83.2	84.7	3.2	3.2	3.8
butanol	0.0	0.0	0.0	0.1	0.0	0.0	5.7	4.6	3.9	96.8	96.8	96.2
						Experiment Run 12						
methanol	94.4	94.4	90.1	22.3	23.3	14.5	0.5	0.7	0.4	0.0	0.0	0.0
ethanol	5.6	5.6	9.9	56.3	60.3	69.8	7.3	10.4	11.9	0.0	0.0	0.0
propanol	0.0	0.0	0.0	21.3	16.4	15.6	86.3	83.6	83.6	2.8	2.8	4.0
butanol	0.0	0.0	0.0	0.1	0.0	0.0	5.9	5.4	4.0	97.2	97.2	96.0

dx.doi.org/10.1021/ie301432z | Ind. Eng. Chem. Res. 2012, 51, 15696−15709

CONCLUSIONS

The experimental studies verify that stable operation of the four product Kaibel column can be achieved with the 4-point temperature control scheme shown in Figure 3c. The control structure gave good servo performance for set point changes as well as good regulation for a +20% feed disturbance. The same control structure was adopted during the cold start-up of the column and with the proposed procedure for adjusting the temperature set points, it was possible to use only temperature measurements to approach the desired steady-state composition, that is, without needing online composition measurements.

An equilibrium stage model was fitted to the experiments. The fitted model gave good match with the experiments. This suggests that equilibrium staged models can be used to study the operation and design of such columns.

APPENDIX

Model Details

The Kaibel column under study is modelled in Matlab using seven column sections.[25] The model is available at the home page of the corresponding author, S. Skogestad. We assume constant pressure, equilibrium on all stages, a total condenser, constant molar flows and linearized liquid dynamics. The model equations for a column sections are

1. Total material balance on stage "i":

$$\frac{\mathrm{d}}{\mathrm{d}t}M_i = L_{i+1} - L_i + V_{i-1} - V_i$$

where M_i is molar holdup on stage "i"; tray numbering is from bottom to top. L_i is liquid molar flow and V_i is total molar vapor flow from a stage "i".

2. Component balance on stage "i" for a component "j":

$$\frac{\mathrm{d}}{\mathrm{d}t}(x_{j,i}M_i) = L_{i+1}x_{j,i+1} + V_{i-1}y_{j,i-1} - L_ix_{j,i} - V_iy_{j,i}$$

where, $x_{j,i}$ is mole fraction of component "j" in liquid phase on stage "i":

3. Vapor−Liquid Equilibria. The VLE is described as

$$Py_j = x_j\gamma_jP_j^S$$

where P is the total pressure and saturation vapor pressures (P^S) is given by Antoine equation:

$$\log P_j^S = A_j - \frac{B_j}{T_i + C_j}$$

where A, B, and C are Antoine constants and T_i is absolute temperature of a stage "i". The ideal vapor phase is assumed, and the Wilson model is used for the liquid phase activity coefficients (γ_i).

4. Constant molar flow in a section:

$$V_{i-1} = V_i = V_{i+1}$$

This assumption holds well since the four components have similar heats of vaporization (35.3, 38.5, 41.8, and 43.1 kJ/kmol) at their normal boiling points.

Linearized flow dynamics:

$$L_i = L_{0,i} + (M_i - M_{0,i})/\tau + V_{i-1} - V_{0,i-1}$$

L_0, V_0, and M_0 are nominal values for molar liquid flows, molar liquid flows, and molar hold up, respectively at time, $t = 0$; $\tau = 0.063$ min.

AUTHOR INFORMATION

Corresponding Author

*E-mail: skoge@ntnu.no.

Present Address

¶Senior Process Engineer, Aker Solutions, Norway.

Notes

The authors declare no competing financial interest.

ACKNOWLEDGMENTS

Ms. Kathinka Qvenild Lystad, Engineer, SINTEF Materials and Chemistry, assisted with the analysis of samples using HPLC.

REFERENCES

(1) Petlyuk, F.; Platonov, V.; Avetlyan, V. Optimum Arrangements in the Fractionating Distillation of Multicomponent Mixtures. *Khim. Prom-st.* **1966**, *42*, 865−868.

(2) Kaibel, G. Distillation Columns with Vertical Partitions. *Chem. Eng. Technol.* **1987**, *10*, 92−98.

(3) Fonyó, Z. Thermodynamic Analysis of Rectification. I. Reversible Model of Rectification. *Int. Chem. Eng.* **1974**, *14*, 18−26.

(4) Fonyó, Z. Thermodynamic Analysis of Rectification. II. Finite Cascade Models. *Int. Chem. Eng.* **1974**, *14*, 203−210.

(5) Petlyuk, F.; Platonov, V.; Slavinskii, D. Thermodynamically Optimal Method for Separating Multicomponent Mixtures. *Int. Chem. Eng.* **1965**, *5*, 555−561.

(6) Petlyuk, F.; Platonov, V. Thermodynamically Reversible Multicomponent Distillation. *Khim, Prom-st.* **1964**, 723−726 (in Russian).

(7) Dejanovic, I.; MatijaŽevic, L.; Halvorsen, I.; Skogestad, S.; Jansen, H.; Kaibel, B.; Olujic. Designing Four-Product Dividing Wall Columns for Separation of a Multicomponent Aromatics Mixture. *Chem. Eng. Res. Des.* **2011**, *89*, 1155−1167.

(8) Kaibel, G. 1984; A distillation column for fractionating multicomponent feed (German Title: Destillationskolonne zur destillativen Zerlegung eines aus mehreren Fraktionen bestehenden Zulaufproduktes), European Patent EP 0 122 367 A2, 1984 (1984); Priority data DE 3302525 (1983).

(9) Halvorsen, I. J.; Skogestad, S. Minimum Energy Consumption in Multicomponent Distillation. 3. More Than Three Products and Generalized Petlyuk Arrangements. *Ind. Eng. Chem. Res.* **2003**, *42*, 616−629.

(10) Olujic, Z.; Jödecke, M.; Shilkin, A.; Schuch, G.; Kaibel, B. Equipment Improvement Trends in Distillation. *Chem. Eng. Process.: PI* **2009**, *48*, 1089−1104.

(11) Dejanovic, I.; Matijaševic, L.; Olujić, Z. Dividing Wall Column, A Breakthrough Towards Sustainable Distilling. *Chem. Eng. Process.: PI* **2010**, *49*, 559−580.

(12) Niggemann, G.; Hiller, C.; Fieg, G. Experimental and Theoretical Studies of a Dividing-Wall Column Used for the Recovery of High-Purity Products. *Ind. Eng. Chem. Res.* **2010**, *49*, 6566−6577.

(13) Niggemann, G.; Gruetzmann, S.; Fieg, G. Distillation Startup of Fully Thermally Coupled Distillation Columns: Theoritical Examination. *Proc. 8th Distill. Absorp., IChemE Symp. Ser.* **2006**, *152*, 800−808.

(14) Mutalib, M. I. A.; Smith, R. Operation and Control of Dividing Wall Distillation Columns: Part 1: Degrees of Freedom and Dynamic Simulation. *Chem. Eng. Res. Des.* **1998**, *76*, 308−318.

(15) Mutalib, M. I. A.; Zeglam, A. O.; Smith, R. Operation and Control of Dividing Wall Distillation Columns: Part 2: Simulation and Pilot Plant Studies Using Temperature Control. *Chem. Eng. Res. Des.* **1998**, *76*, 319−334.

(16) Ling, H.; Luyben, W. L. New Control Structure for Divided-Wall Columns. *Ind. Eng. Chem. Res.* **2009**, *48*, 6034−6049.
(17) van Diggelen, R. C.; Kiss, A. A.; Heemink, A. W. Comparison of Control Strategies for Dividing-Wall Columns. *Ind. Eng. Chem. Res.* **2010**, *49*, 288−307.
(18) Ling, H.; Cai, Z.; Wu, H.; Wang, J.; Shen, B. Remixing Control for Divided-Wall Columns. *Ind. Eng. Chem. Res.* **2011**, *50*, 12694−12705.
(19) Adrian, T.; Schoenmakers, H.; Boll, M. Model predictive control of integrated unit operations: Control of a divided wall column. *Chem. Eng. Process.* **2004**, *43*, 347−355.
(20) Rewagad, R. R.; Kiss, A. A. Dynamic optimization of a dividing-wall column using model predictive control. *Chem. Eng. Sc.* **2012**, *68*, 132−142.
(21) Buck, C.; Hiller, C.; Fieg, G. Applying Model Predictive Control to Dividing Wall Columns. *Chem. Eng. Technol.* **2011**, *34*, 663−672.
(22) Strandberg, J.; Skogestad, S. Stabilizing Control of an Integrated 4-Product Kaibel Column. *Proc. IFAC Int. Symp. Advan. Control Chem. Proc. (ADCHEM 2006)*, **2006**, *2*, 623−628.
(23) Ghadrdan, M.; Halvorsen, I. J.; Skogestad, S. Optimal Operation of Kaibel Distillation Columns. *Chem. Eng. Res. Des.* **2011**, *89*, 1382−1391.
(24) Kvernland, M.; Halvorsen, I. J.; Skogestad, S. Model Predictive Control of a Kaibel Distillation Column. *Proc. 9th Int. Symp. DYCOPS 2010* **2010**, 539−544.
(25) Strandberg, J. Optimal operation of dividing wall columns. Ph.D. Thesis, Norwegian University of Science and Technology, Department of Chemical Engineering, Trondheim, Norway, 2011.
(26) Skogestad, S. Simple Analytic Rules for Model Reduction and PID Controller Tuning. *J. Process Contr.* **2003**, *13*, 291−309.